Carbohydrate Research, 248 (1993) 15–36
Elsevier Science Publishers B.V., Amsterdam

The conformation of the monomethyl ethers of methyl β-lactoside in D_2O and Me_2SO-d_6 solutions

Paloma Fernández and Jesús Jiménez-Barbero

Grupo de Carbohidratos, Instituto de Química Orgánica General, Juan de la Cierva 3, 28006 Madrid (Spain)

(Received January 4th, 1993; accepted April 26th, 1993)

ABSTRACT

The solution conformations of all the possible monomethyl ethers of methyl β-lactoside have been analysed using molecular mechanics and dynamics calculations and nuclear magnetic resonance data (variable temperature and NOE experiments). The overall shape of all the compounds studied is fairly similar and may be described by conformers included in a low-energy region with $\Phi = -100 \pm 40°$ and $\Psi = -135 \pm 35°$, which is ca. 5% of the total potential energy surface for the glycosidic linkages of the disaccharides.

INTRODUCTION

We have reported on the recognition of methyl β-lactoside[1] (**1**) and its monodeoxy derivatives by the β-galactoside-specific lectins ricin (RCA 60) and agglutinin (RCA 120), isolated from *Ricinus communis* seeds[1,2]. On the basis of the dissociation constants observed, we have suggested that the glucose moiety having a $^4C_1$ chair conformation is involved in the recognition, and have proposed the existence of a hydrophobic interaction between the lectins and the C-3 region of the disaccharide, while HO-3′, HO-4′, and HO-6′ are involved in hydrogen bonding to the protein. Besides, a smaller polar interaction between HO-2′ and the receptors seems to be operative.

It is accepted that the total hydrogen-bonding donor and acceptor capacity of a hydroxyl group to interact with a protein group may be assessed by using a deoxy analogue[3]. However, the separation of the energetic contributions of the donor and acceptor components is a more difficult task and has usually been proved through the use of deoxyfluoro[4] or *O*-methyl derivatives[5], although the use of the former compounds has been disputed[6]. The use of *O*-methyl derivatives has recently been recommended[7], since they may not only give an answer to the accepting capacity of a given hydroxyl group, but also may predict the position of the recognition site in the periphery or the interior of the protein. A study of the recognition phenomenon based on modified substrates must be accompanied by

0008-6215/93/$06.00 © 1993 – Elsevier Science Publishers B.V. All rights reserved

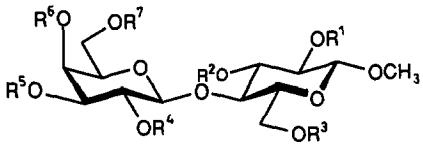

1 R^1-R^7 =H

2 R^1 =Me, R^2-R^7 =H

3 R^1 =H, R^2 =Me, R^3-R^7 =H

4 R^1 =R^2 =H, R^3 =Me, R^4-R^7 =H

5 R^1-R^3 =H, R^4 =Me, R^5-R^7 =H

6 R^1-R^4 =H, R^5 =Me, R^6 =R^7 =H

7 R^1-R^5 =H, R^6 =Me, R^7 =H

8 R^1-R^6 =H, R^7 =Me

the analysis of the possible changes in their three-dimensional structure in order to be able to correlate structure and activity. On this basis, we now report on the conformational analysis of all the possible monomethyl ethers (**2–8**) of methyl β-lactoside in D_2O and Me_2SO-d_6 solutions, based on molecular mechanics and dynamics calculations, and NMR data, particularly variable temperature experiments and proton NOE measurements, in order to test the possible changes in the three-dimensional shape of the disaccharides upon *O*-methylation of the different hydroxyl groups. These compounds have been used as ligands for ricin and agglutinin[8]. A previous study of the conformation of methyl β-lactoside bound to ricin-B showed[9] that the conformational changes between the free and the bound ligands were slight. On the other hand, a recent report on the conformation of methyl melibioside bound to ricin-B led to the conclusion[10] that the usually flexible α-(1 → 6) linkage in this α-(1 → 6)-linked disaccharide is frozen in one of its potential conformations upon binding to the lectin, and that the glucose part is not involved in the binding. Nevertheless, it has to be noted that the spatial position of the glucose ring with respect to the galactose moiety in the β-(1 → 4) and the α-(1 → 6) linkages is rather different.

EXPERIMENTAL

Materials.—Compounds **2–8** were prepared in our laboratory and their syntheses will be reported elsewhere.

NMR experiments.—NMR spectra were recorded at 37°C in D_2O, and at 37°C and 60°C in Me_2SO-d_6, with a Varian Unity 500 spectrometer. Proton chemical shifts were referenced to residual HDO at δ 4.64 ppm or residual Me_2SO-d_6 at δ

2.49 ppm. Carbon chemical shifts were referenced to external 1,4-dioxane at δ 67.4 ppm.

The double quantum filtered DQF-COSY experiments were performed in the phase-sensitive mode using the standard Varian sequence. A data matrix of $256 \times 2K$ points was used to digitize a spectral width of 1500 Hz. 16 Scans were used per increment with a relaxation delay of 2 s. The 90° pulse width was 7.5 μs. Prior to Fourier transformation, zero-filling was used in F_1 to expand the data to $1K \times 2K$.

The clean 2D-TOCSY experiments[11] were carried out in the phase-sensitive mode using MLEV-17 for isotropic mixing. The mixing time was set to 150 ms. A data matrix of $256 \times 1K$ points was used to digitize a spectral width of 1500 Hz. 16 Scans were used per increment with a relaxation delay of 2 s. The 90° pulse width during the mixing period was 22.5 μs. Squared cosine-bell functions were applied in both dimensions and zero-filling was used to expand the data to $2K \times 2K$.

The 2D rotating frame NOE (ROESY, CAMELSPIN) experiments were recorded[12] in the phase sensitive mode. The spin-lock period consisted of a train of 30° pulses (2.5 μs), separated by delays of 50 μs. The total mixing time was set to 350 ms. The rf carrier was set at δ 5.5 ppm to minimize spurious Hartmann–Hahn effects[12,13]. A data matrix of $256 \times 2K$ points was used to resolve a spectral width of 3000 Hz. 32 Scans were used per increment with a relaxation delay of 2 s. Prior to Fourier transformation, squared sine-bell functions shifted by $\pi/3$ were applied in both dimensions and zero-filling was used in F_1 to expand the data to $2K \times 2K$.

The pure absorption 2D-NOESY experiments were carried out with mixing times of 200, 350, and 700 ms. A data matrix of $256 \times 2K$ points was used to resolve a spectral width of 1500 Hz. 32 Scans were used per increment with a relaxation delay of 2 s. Prior to Fourier transformation, squared sine-bell function shifted by $\pi/3$ were applied in both dimensions and zero-filling was used in F_1 to expand the data to $2K \times 2K$. NOESY and ROESY were integrated using standard Varian software after applying a third-order polynomial baseline correction in both dimensions. The total intensity of the added ω_1 cross-sections containing diagonal and cross-peaks was given a 100% value[14]. The steady-state NOE experiments were performed through the interleaved differential technique using a saturation delay of 7 s. Between 256 and 512 free induction decays were accumulated for each irradiation site.

The pure absorption one-bond proton–carbon correlation experiments were collected in the ^{1}H-detection mode using the HMQC or HSMQC pulse sequences[15] and a reverse probe. A data matrix of $256 \times 2K$ points was used to resolve a spectral width of 1500 Hz. 16 Scans were used per increment with a relaxation delay of 1 s and a delay corresponding to a J value of 152 Hz. A BIRD-pulse was used to minimize the proton signals bonded to ^{12}C. ^{13}C-Decoupling was achieved by the WALTZ scheme. Prior to Fourier transformation, squared cosine-bell functions were applied in both dimensions and zero-filling was used in F_1 to expand the data to $2K \times 2K$.

The pure absorption HSMQC-ROESY experiments were collected in the ^{1}H-detection mode using the pulse sequence 90(^{1}H)–Δ–90(^{1}H, ^{13}C)–$t_1/2$–180(^{1}H)–$t_1/2$–90(^{1}H, ^{13}C)–Δ–spinlock–acq(^{1}H), where Δ is $1/2J_{CH}$ and the spin lock time was set to 300 ms. The phase cycling was based on the combination of the original HSMQC[15b] and ROESY[12] pulse sequences. A data matrix of 128 × 2K points was used to resolve a spectral width of 8000 and 2000 Hz in F_1 and F_2, respectively. The carrier was set 100 Hz downfield from the most deshielded proton resonance. 256 Scans were used per increment with a relaxation delay of 1 s and a Δ delay corresponding to a J value of 150 Hz. A BIRD-pulse was used to minimize the proton signals bonded to ^{12}C. ^{13}C-Decoupling was not used during acquisition. Prior to Fourier transformation, squared cosine-bell functions were applied in both dimensions and zero-filling was used to expand the data to 2K × 4K.

^{13}C NMR spin–lattice relaxation times were determined for compounds **3**, **5**, and **6** in D_2O at 37°C and in Me_2SO-d_6 at 37 and 60°C through the inversion recovery technique using Varian software. Two independent sets of eight delays were used in the determination. The T_1 values were used to estimate the average correlation time (τ_c) of these molecules at the different temperatures, assuming isotropic motion and dipole–dipole relaxation only.

Molecular mechanics and dynamics calculations.—The MM2 low-energy conformers found previously[1] for **1** (A, B, C/C′, D, E) were modified by adding a methyl group at the desired position and submitted to further minimization. Dihedral angles at the glycosidic linkages are defined as Φ O-5′, C-1′, O-1′, C-4 and Ψ C-1′, O-1′, C-4, C-5. Only the *gt* conformation of the lateral chain was used for the galactose residue, while both the *gg* and *gt* rotamers were considered for the glucose moiety[16]. In all cases, both Φ and Ψ angles remained close (ca. ±5°) to the starting point. A dielectric constant of 1.5 D was used. The geometries of compound **1** describing minima A, D, and E (*gg* for the glucose residue) were then taken as starting structures for molecular dynamics (MD) calculations in vacuo by using the CVFF[17] and Discover 2.8 programs[18]. The MD simulations were performed at 303 K with a dielectric constant of 78 D and a time step of 1 fs. The equilibration time was 20 ps and the total simulation time was 520 or 1020 ps. Trajectory frames were saved every 0.5 ps. Additional MD simulations were carried out for compounds **3** and **5**, but only the corresponding A conformer (*gg* for the glucose residue) was chosen as starting geometry. The trajectories were examined with the Analysis module of INSIGHT II[19].

The steady-state 1D-NOE and the 2D-NOE experiments were calculated according to the complete relaxation matrix method[20] by using the NOEMOL program[21] for the geometries of conformers A, B, C, and C′, and for a Boltzmann distribution of these minima, calculated from the MM2 relative energies. Isotropic motion and no external relaxation was assumed in the calculation process. Since NOEs are extremely dependent on the correlation time used for the calculation, different τ_c values were tested in order to get the best match between the experimental and the calculated NOE for a given intraresidue proton pair. ROESY

experiments were used to estimate interproton distances according to the isolated spin-pair approximation[22].

RESULTS AND DISCUSSION

Table I shows the values of the estimated populations of the different conformers obtained by MM2 optimisation of the HSEA minima obtained previously[1] for **1**, along with those obtained by use of the Discover–CVFF programme. These calculated energies should be taken as approximate since they are variable at least 0.5 kcal/mol. The predicted distribution of conformers estimated from the relative energy values is also given in Table I. A Ramachandran-type plot of the isoenergy contour is given in Fig. 1. It can be observed that there are six local minima under a level of relative steric energy of ca. 3.50 kcal, while there is a broad low-energy region described by conformers A, B, C, and C′ with rather small energy barriers among them[1]. Figs. 2 and 3 show stereoscopic views of these low-energy conformers along with their corresponding Φ and Ψ values. The previously reported X-ray structures for different β-(1 → 4) equatorial-linked disaccharides are included in this low-energy region[1]. According to the calculations, this low-energy region described by $\Phi = -100 \pm 40°$, $\Psi = -135 \pm 35°$, and $r_{H\text{-}1'-H\text{-}4} = 2.4 \pm 0.4$ Å appears to be populated to more than 95% extent while the two islands described by conformers D and E are populated less than 5% at 37 or 60°C. Nevertheless, the possibility of their existence in solution should be investigated since the conformation of some synthetic interglycosidic acetals of lactose and cellobiose[23] is that of conformer D, while very recently, the X-ray analysis of the bound conformation of

TABLE I

Estimated Populations (%) for the low-energy conformers of **1**, **3–5**, and **8** estimated from the MM2 [a] and CVFF [b] steric energy values

Compound	Conformer				
	A	B	C/C′ [c]	D	E
	Population [a]				
1	33.9	37.8	26.3	1.8	0.2
3	45.5	37.5	15.0	1.7	0.3
4	36.0	32.3	29.7	1.7	0.3
5	32.7	31.3	33.5	1.9	0.6
8	32.5	35.5	30.0	1.7	0.3
	Conformer				
	A	B	C/C′	D	E
	Population [b]				
1	36.1	31.2	31.0	1.4	0.3

[a] From MM2 energy values. [b] From CVFF energy values. [c] Minimum C shows *gt* orientation for the C-5–C-6 torsion angle of the glucopyranose ring, while conformer C′ shows *gg* orientation for the C-5–C-6 torsion angle of the glucopyranose ring.

a biantennary octasaccharide to *Lathyrus ochrus* isolectin I has shown the presence of a β-Man-(1 → 4)-GlcNAc linkage in conformation E, and a β-Gal-(1 → 4)-GlcNac moiety located in island D[24,25]. The stability of the different conformations was tested by using molecular dynamics simulations with the use of the Discover–CVFF program. Although the CVFF is a general MD program not specifically parametrized for oligosaccharides, and therefore does not include any potential for the exo-anomeric effect[26], its use in the conformational analysis of different oligosaccharides has produced satisfactory results[27]. The minimized A, D, and E conformations were used as input geometries for different 520-ps simulations at 303 K. The trajectories of the simulations are displayed in Fig. 4. No chair-to-chair or chair-to-boat interconversions were observed. The average Φ and Ψ angles were -84 ± 5 and $-135 \pm 5°$, depending on the starting conformation. After the corresponding equilibration periods (ca. 20 ps), it was observed that the simulations remained most of the time (> 95%) in the low-energy region described by conformers A, B, C, and C′. In fact, only when the simulation started from conformer D was there a significant occupancy of this region for ca. 40 ps, although the trajectory moved again to the broad low-energy region. Even when the starting geometry was that of conformer E, the simulation resulted in a transition to region A-C′ almost immediately. Therefore, these results seem to indicate that conformers D and E are not stable enough to complete with A-C′, when such external factors as stabilization by hydrogen or covalent bonds or non-polar contacts are not operating[24]. The 520-ps simulation for compound **5** (2′-*O*-methyl) produced basically the same results, the Φ and Ψ angles oscillating between -60 and $-140°$, and -120 and $-170°$, respectively. The methyl group at position O-2′ also showed important oscillations around the C–O bond. However,

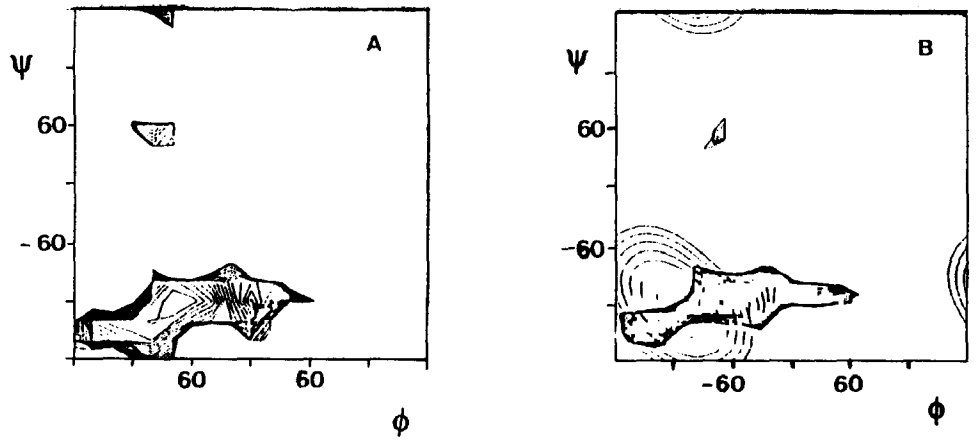

Fig. 1. A Ramachandran-type plot of the isoenergy contours of compounds **1** (**A**) and **3** (**B**) calculated by the CVFF programme. Plot **B** also shows the region defined by distances H-1′–H-4 between 2.1 and 2.5 Å.

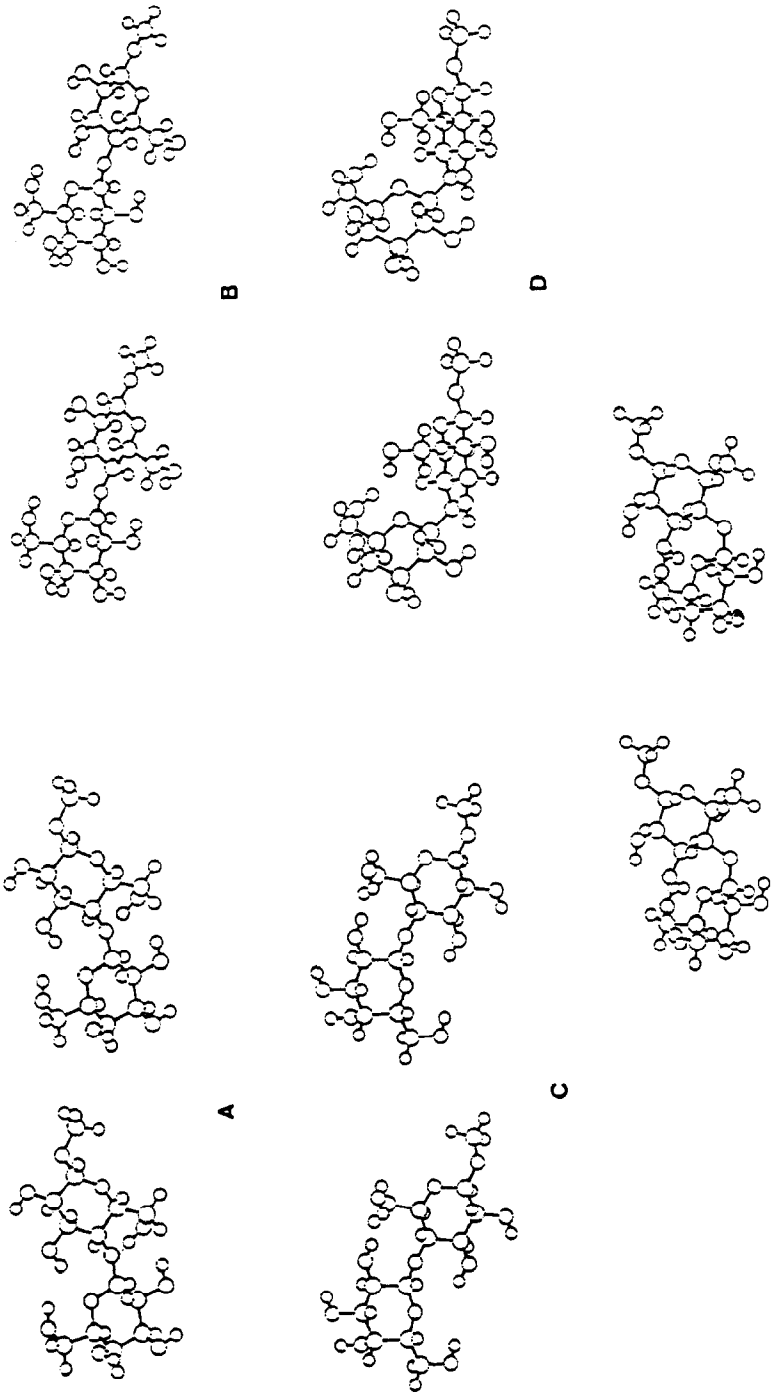

Fig. 2. Stereoscopic views of the low-energy conformers of compound **1**. **A**, conformer A, Φ −70, Ψ −116; **B**, conformer B, Φ −96, Ψ −176; **C**, conformer C, Φ −150, Ψ −156; **D**, conformer D, Φ −92, Ψ 61; **E**, conformer E, Φ 60, Ψ −122.

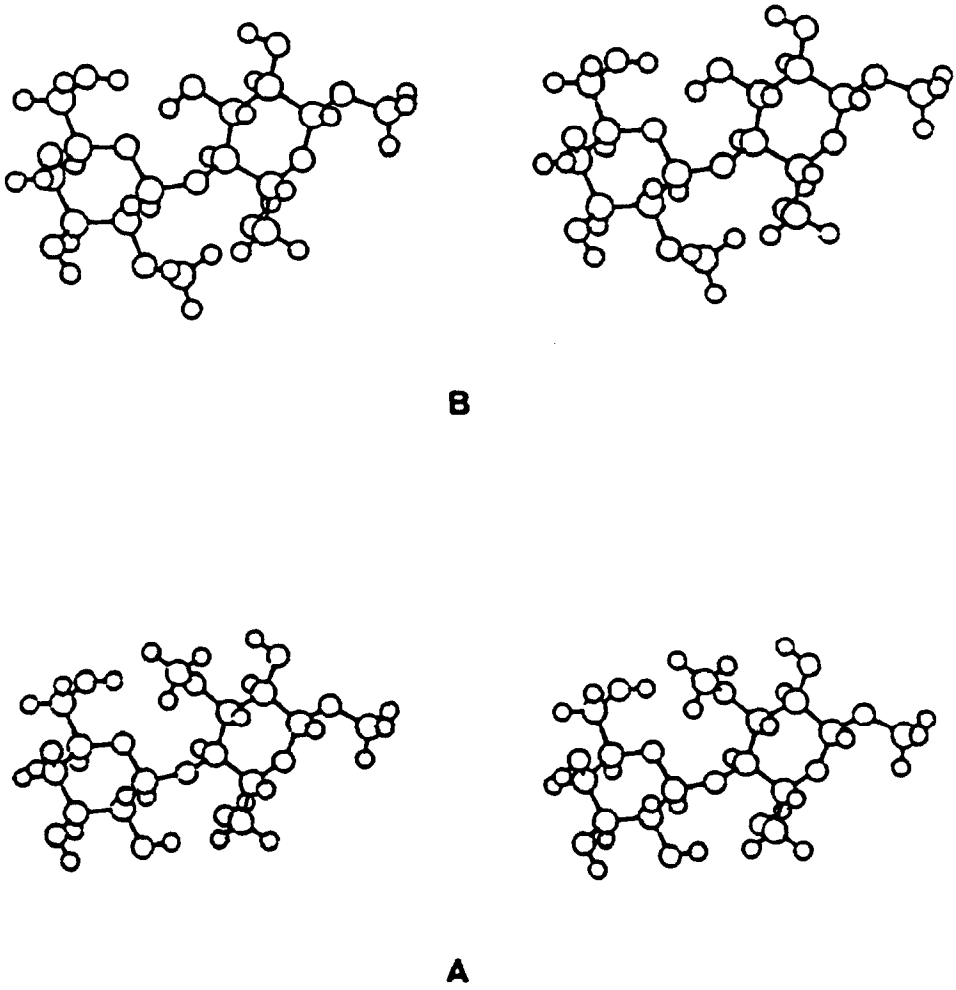

Fig. 3. Stereoscopic views of conformer A of compounds **3** (**A**) and **5** (**B**).

the same simulation for the 3-*O*-methyl derivative **3** showed the smallest degree of fluctuations around the glycosidic bond after an initial period of 50 ps (Fig. 5). The lack of fluctuations was also noticeable in a different 1000-ps simulation. Also, the oscillations around the O-3–C-3 bond were highly diminished after 50 ps, independently of the starting orientation for that *O*-methyl group. A similar rigidity has recently been observed[26b,28] for the Le^x trisaccharide, which presents a fucosyl group at position O-3 of the lactosamine moiety. In all cases, several transitions between the *gg*, *gt*, and *tg* orientations of the lateral chains were observed.

NMR spectroscopy can be used either qualitatively or quantitatively to distinguish the presence of either conformer[29]. All of the low-energy region described by minima A, B, C, C′ shows short distances between H-4 and H-1′; H-3 stands close to H-1′ in conformer E, H-4 is close to H-2′ in conformer D, and there is a unique

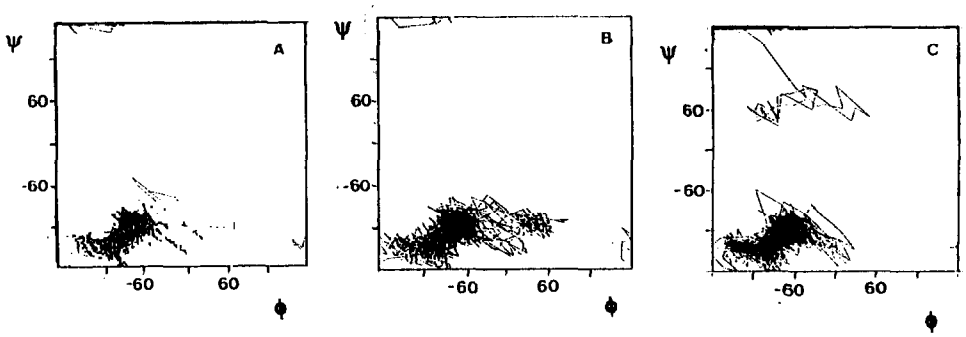

Fig. 4. Contour plots of the trajectories (500 ps) calculated from molecular dynamics simulations for compound **1**, starting from coordinates corresponding to **A**, conformer A; **B**, conformer D; and **C**, conformer E.

contact between H-1′ and H-6*pro-R* (H-6_R) or H-6*pro-S* (H-6_S) for the *gg* or *gt* rotamers of conformer A, respectively. Conformers A and B can be stabilized by formation of a hydrogen bond between HO-3 and O-5′ since both oxygen atoms are less than 2.9 Å apart. These structural characteristics along with others involving oxygen atoms are collected in Table II. The existence of one or two interresidue NOEs and of some specific shieldings or deshieldings imposes con-

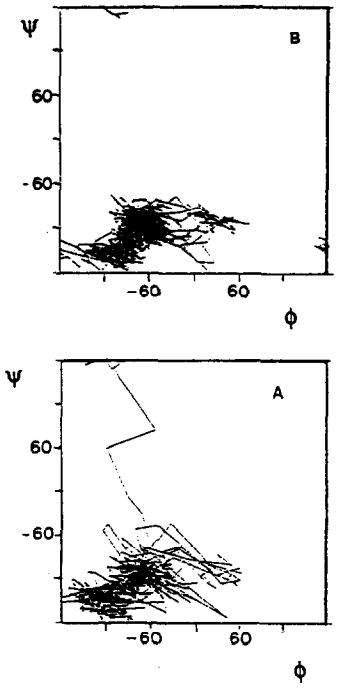

Fig. 5. Contour plots of the trajectories (500 ps) calculated from molecular dynamics simulations for compounds **3** (**A**) and **5** (**B**) starting from coordinates corresponding to conformer A.

TABLE II

Relevant interatomic distances for the low-energy conformers of **1–8**

Distance (Å)	Conformer (Φ/Ψ)				
	A	B	C/C′	D	E
	Φ(°)				
	−70	−96	−140/−113	60	−92
	Ψ (°)				
	−116	−175	−150/−161	−122	61
H-1′–H-4	2.33	2.34	2.23	> 3.5	> 3.5
H-1′–H-3	> 3.5	> 3.5	> 3.5	> 3.5	1.79
H-1′–H-5	> 3.5	> 3.5	> 3.5	> 3.5	2.23
H-1′–H-6_R	2.49 [a]	> 3.5	> 3.5	> 3.5	> 3.5
H-1′–H-6_S	2.52 [b]	> 3.5	> 3.5	> 3.5	> 3.5
H-1′–O-3	> 3.5	2.48	2.47	> 3.5	> 3.5
H-1′–O-6	2.52	> 3.5	> 3.5	> 3.5	> 3.5
H-2′–H-4	> 3.5	> 3.5	> 3.5	1.94	> 3.5
O-2′–O-3	> 3.5	> 3.5	> 3.5	2.93	> 3.5
O-5′–O-3	3.02	2.63	3.06	> 3.5	> 3.5
O-2′–H-6_R	2.96 [a]	> 3.5	3.12	> 3.5	> 3.5
O-2′–H-6_S	2.99 [b]	> 3.5	3.06	> 3.5	> 3.5

[a] *gg* or [b] *gt* rotamer around the C-5–C-6 bond.

straints in the conformational map and can indicate the presence of a given conformer[29,30]. The combination of homo and hetero 2D-NMR techniques allows the unambiguous assignment of all the resonances of compounds **1–8**. Particularly useful were the ^{1}H-detected HMQC and HSMQC experiments to resolve the cases of overlapping resonances. The first-order chemical shifts and relevant coupling constants for compounds **1–8** are shown in Tables III–VIII.

No important chemical shift differences were detected between **1** and compounds **2–8** in D_2O solution, apart from those expected for specific *O*-methyl substitution (see below). Some long-range effects are observed for compounds **4** (6-*O*-methyl) ($\Delta\delta_{H\text{-}1'} = -0.06$ ppm) and **3** (3-*O*-methyl) ($\Delta\delta_{H\text{-}5'} = -0.06$ ppm). Besides, *H-6pro-R* is slightly affected by the substitution at O-2′ ($\Delta\delta = -0.04$ ppm). These effects are also observed in Me_2SO-d_6, with shieldings of 0.08, 0.14, and 0.03 ppm for H-1′ of **4**, H-5′ of **3**, and H-6*pro-R* of **5**, respectively. It can also be observed that in Me_2SO-d_6, the methylation at O-3 produces a deshielding of H-1′ (0.10 ppm) and a small shielding of the H-2′ resonance (0.04 ppm). All these data agree with an important presence of conformers in the A/B region (Table II). The ^{1}H NMR chemical shifts for the hydroxyl protons in Me_2SO-d_6 at 30°C and the differences between these values and those determined at 70°C are given in Table VIII. These differences are smaller for HO-3 than for any other hydroxyl group in this set of compounds. Moreover, the $J_{HO\text{-}3,H\text{-}3}$ values were always < 1.5 Hz, indicating an average dihedral angle close to 90° and a particular orientation for that proton, while the remaining vicinal couplings involving hydroxyl groups were ca. 6–7 Hz, as expected for an almost freely rotating hydroxyl group. Thus, as

TABLE III

^{1}H NMR chemical shifts (δ, ppm) for compounds **1–8** in D_2O solution at 37°C

Proton	Compound							
	1	**2**	**3**	**4**	**5**	**6**	**7**	**8**
Glucose residue								
H-1	4.40	4.43	4.39	4.37	4.39	4.41	4.41	4.39
H-2	3.30	3.06	3.37	3.29	3.29	3.31	3.31	3.30
H-3	3.64	3.67	3.45	3.63	3.63	3.63	3.64	3.65
H-4	3.63	3.66	3.79	3.63	3.64	3.66	3.61	3.64
H-5	3.59	3.57	3.56	3.67	3.59	3.65	3.61	3.60
H-6_S	3.98	3.98	4.00	3.81	3.97	4.00	3.99	3.98
H-6_R	3.80	3.78	3.82	3.72	3.76	3.82	3.81	3.80
Galactose residue								
H-1′	4.44	4.45	4.45	4.38	4.47	4.47	4.41	4.44
H-2′	3.53	3.53	3.52	3.53	3.25	3.57	3.49	3.54
H-3′	3.65	3.64	3.65	3.66	3.66	3.37	3.72	3.67
H-4′	3.92	3.92	3.92	3.92	3.91	4.17	3.63	3.91
H-5′	3.72	3.71	3.66	3.70	3.75	3.72	3.74	3.87
H-$6'_R$	3.78	3.77	3.80	3.78	3.79	3.80	3.81	3.86
H-$6'_S$	3.75	3.74	3.75	3.74	3.74	3.79	3.64	3.65
O-CH_3 [a]	3.56	3.58	3.56	3.56	3.58	3.56	3.56	3.56
O-CH_3 [b]		3.58	3.60	3.39	3.56	3.35	3.51	3.39

[a] Reducing end. [b] Substitution at given position.

TABLE IV

^{1}H NMR chemical shifts (δ, ppm) for compounds **1–8** in Me_2SO-d_6 solution at 37°C

Proton	Compound							
	1	**2**	**3**	**4**	**5**	**6**	**7**	**8**
Glucose residue								
H-1	4.09	4.18	4.07	4.09	4.09	4.09	4.08	4.09
H-2	3.00	2.76	3.07	2.99	3.00	3.01	2.99	2.99
H-3	3.32	3.39	3.10	3.30	3.29	3.30	3.29	3.28
H-4	3.29	3.30	3.49	3.23	3.29	3.28	3.28	3.27
H-5	3.28	3.27	3.23	3.42	3.28	3.29	3.27	3.27
H-6_S	3.74	3.75	3.73	3.71	3.72	3.74	3.74	3.75
H-6_R	3.60	3.59	3.66	3.54	3.57	3.60	3.59	3.66
Galactose residue								
H-1′	4.19	4.17	4.29	4.11	4.24	4.22	4.19	4.21
H-2′	3.31	3.29	3.27	3.31	3.02	3.43	3.27	3.32
H-3′	3.30	3.28	3.27	3.29	3.38	3.02	3.40	3.32
H-4′	3.61	3.62	3.63	3.63	3.60	3.87	3.37	3.56
H-5′	3.45	3.44	3.31	3.44	3.41	3.44	3.47	3.64
H-$6'_R$	3.51	3.52	3.57	3.53	3.53	3.57	3.50	3.46
H-$6'_S$	3.46	3.48	3.47	3.46	3.50	3.49	3.45	3.42
O-CH_3 [a]	3.38	3.40	3.37	3.37	3.38	3.39	3.38	3.38
O-CH_3 [b]		3.42	3.45	3.27	3.42	3.31	3.42	3.25

[a] Reducing end. [b] Substitution at a given position.

TABLE V

^{13}C NMR chemical shifts (δ, ppm) for compounds **1–8** in D_2O solution at 37°C

Carbon	Compound							
	1	**2**	**3**	**4**	**5**	**6**	**7**	**8**
Glucose residue								
C-1	104.3	104.1	104.0	104.3	104.3	104.3	104.4	104.3
C-2	74.1	83.5	73.3	74.0	74.1	74.0	74.1	74.1
C-3	75.8	75.1	84.7	75.6	75.6	75.6	75.8	76.0
C-4	79.9	79.5	76.7	79.5	79.7	79.5	79.8	80.4
C-5	76.1	75.9	76.4	74.7	76.2	76.0	76.1	75.8
C-6	61.4	61.3	61.1	71.5	61.4	61.2	61.5	61.5
Galactose residue								
C-1′	104.4	104.2	104.3	104.4	104.0	104.1	104.2	104.3
C-2′	72.3	72.2	72.5	72.2	82.2	71.2	72.6	72.4
C-3′	73.9	73.8	73.9	73.8	73.6	82.9	74.3	73.8
C-4′	69.9	69.3	69.8	69.8	69.9	65.4	80.3	72.7
C-5′	76.7	76.6	76.5	76.6	76.5	76.5	76.9	74.4
C-6′	62.3	62.3	62.2	62.3	62.3	62.3	61.9	70.0
O-CH_3 [a]	58.4	58.4	58.2	58.6	58.5	58.4	58.6	58.5
O-CH_3 [b]		61.2	60.2	59.7	61.9	57.5	62.8	59.7

[a] Reducing end. [b] Substitution at a given position.

previously stated[31] for the deoxy analogues of **1**, HO-3 of compounds **1**, **2** and **4–8** in Me_2SO-d_6 solution participates in interresidue hydrogen bonding, probably with O-5′, as occurs in the crystal of β-lactose[32] and has been recently demonstrated in a detailed study[33] of methyl β-cellobioside in Me_2SO-d_6.

TABLE VI

^{13}C NMR chemical shifts (δ, ppm) for compounds **1–8** in Me_2SO-d_6 solution at 37°C

Carbon	Compound							
	1	**2**	**3**	**4**	**5**	**6**	**7**	**8**
Glucose residue								
C-1	105.5	105.0	105.9	105.4	105.4	105.5	105.5	105.5
C-2	75.1	85.0	75.6	75.0	75.0	75.0	75.1	75.0
C-3	76.7	76.3	87.1	76.7	76.8	76.7	76.7	76.7
C-4	82.5	82.7	78.5	82.3	82.3	82.6	82.3	82.7
C-5	76.8	76.5	77.3	75.5	77.0	76.7	77.0	76.9
C-6	62.3	62.2	62.3	72.6	62.2	62.3	62.3	62.4
Galactose residue								
C-1′	105.7	105.8	105.8	105.9	105.0	105.6	105.5	105.6
C-2′	72.4	72.4	73.7	72.4	83.0	71.3	72.8	72.4
C-3′	75.0	75.1	75.1	75.2	74.6	84.8	75.7	75.0
C-4′	70.0	70.0	70.0	70.0	70.3	65.5	80.2	70.5
C-5′	77.4	77.5	77.4	77.4	77.3	77.3	76.7	75.2
C-6′	62.4	62.3	62.4	62.3	62.2	62.2	61.6	73.7
O-CH_3 [a]	58.1	58.1	58.2	58.0	57.9	58.0	58.0	58.0
O-CH_2 [b]	–	61.7	61.4	60.3	62.0	58.2	62.3	60.3

[a] Reducing end. [b] Substitution at a given position.

TABLE VII

^{1}H NMR vicinal coupling constants (J, Hz) for the lateral chains of the glucose and galactose residues of compounds **1–8** in D_2O and Me_2SO-d_6 solutions at 37°C, and estimated populations of the different rotamers *gg*, *gt*, and *tg*

$^3J_{H,H}$	Compound							
	1	**2**	**3**	**4**	**5**	**6**	**7**	**8**
Glucose residue								
D_2O								
$J_{5,6S}$	2.3	2.3	2.3	1.6	2.1	2.3	2.0	1.6
$J_{5,6R}$	5.2	5.1	5.3	5.0	3.7	5.2	5.0	4.7
%*gg*	60	60	60	65	70	60	60	65
%*gt*	40	40	40	35	30	40	40	35
Me_2SO-d_6								
$J_{5,6S}$	2.2	2.4	2.2	2.0	2.1	2.2	2.1	1.7
$J_{5,6R}$	5.1	5.5	5.2	5.3	4.6	4.6	4.4	4.5
%*gg*	60	55	60	60	65	65	65	65
%*gt*	40	45	40	40	35	35	35	35
Galactose residue								
D_2O								
$J_{5',6'S}$	4.0	3.6	4.5	4.0	4.4	3.9	4.5	4.6
$J_{5',6'R}$	8.2	7.8	7.6	8.5	7.9	7.7	6.5	8.1
%*tg*	30	35	35	30	35	10	30	35
%*gt*	70	55 [a]	65	70	65	75 [a]	50 [a]	65
Me_2SO-d_6								
$J_{5',6'S}$	4.0	5.1	6.0			4.6		4.5
$J_{5',6'R}$	8.2	7.9	7.5			7.7		7.5
%*tg*	30	35	45				35	35
%*gt*	70	65	55				65	65

[a] There is a participation of the *gg* rotamer.

O-Methyl orientation.—The effect of *O*-methylation on chemical shifts in ^{1}H and ^{13}C NMR spectra of cyclic polyols has been studied by Angyal and Odier[34]. The observed methylation shifts for **2–8** when compared to **1** agree semiquantitatively with their observations. Thus, the *O*-methyl group at position C-2 of both Glc and Gal residues seems to be in equilibrium among its three possible rotamers, as expected when the adjacent carbon atoms carry equatorial substituents. The deshielding of H-1(H-1′) and H-3(H-3′) of **2(5)** is approximately the same in D_2O (0.02–0.03 ppm), while it is larger (0.05–0.09 ppm) in Me_2SO-d_6 and closer to that expected (0.07 ppm). The shielding of H-2 of **2** is 0.24 ppm for both solvents, while H-2′ of **5** is shielded 0.28 and 0.29 ppm in D_2O and Me_2SO-d_6, respectively. According to Angyal and Odier[34], the expected shift is ca. 0.22 ppm. On the other hand, there is a slight shielding of the corresponding C-1 and C-3 signals of ca. 0.3 ppm. The observed shielding due to *O*-methylation lies between 8.9 and 10.6 ppm, as expected. The effect on C-3 of methylation is rather different, since O-4 is also substituted and thus steric conflicts may occur: H-2 is slightly deshielded (0.07 ppm) in both solvents. On the other hand, H-4 is deshielded to a larger extent: 0.16 in D_2O and 0.20 ppm in Me_2SO-d_6. Besides, a long range effect is observed for

TABLE VIII

^{1}H NMR chemical shifts (δ, ppm) and chemical shift differences ($\Delta\delta$) between 30 and 70°C for the hydroxyl protons of **1–8** in Me_2SO-d_6

Compound		Hydroxyl proton						
		HO-2	HO-3	HO-6	HO-2′	HO-3′	HO-4′	HO-6′
1	δ	5.12	4.63	4.53	5.04	4.73	4.46	4.61
	$\Delta\delta$	0.27	0.08	0.21	0.21	0.26	0.21	0.18
2	δ		4.69	4.56	5.05	4.75	4.47	4.65
	$\Delta\delta$		0.09	0.21	0.20	0.24	0.20	0.18
3	δ	5.12		4.45	4.93	4.64	4.31	4.66
	$\Delta\delta$	0.27		0.26	0.29	0.29	0.27	0.25
4	δ	5.12	4.63		5.05	4.75	4.47	4.61
	$\Delta\delta$	0.27	0.08		0.24	0.25	0.21	0.18
5	δ	5.12	4.49	4.58		4.88	4.58	4.63
	$\Delta\delta$	0.27	0.09	0.23		0.23	0.22	0.17
6	δ	5.12	4.59	4.52	5.15		4.52	4.65
	$\Delta\delta$	0.27	0.07	0.20	0.21		0.23	0.19
7	δ	5.12	4.53	4.53	5.09	4.89		4.72
	$\Delta\delta$	0.27	0.07	0.21	0.24	0.25		0.19
8	δ	5.12	4.55	4.53	5.09	4.80	4.59	
	$\Delta\delta$	0.27	0.07	0.21	0.21	0.25	0.22	

H-5′, which is shielded 0.04 in D_2O and 0.14 ppm in Me_2SO-d_6. H-3 is shielded 0.19 and 0.22 ppm in D_2O and Me_2SO-d_6, respectively. The effect on ^{13}C NMR chemical shifts is also important: C-2 varies −0.8 ppm and 0.5 ppm, while C-4 is shielded 3.2 and 4.0 ppm, in D_2O and Me_2SO-d_6, respectively. These shifts seem to indicate that there is some sort of interaction between the methyl group and the galactose moiety. As stated above, according to the MD simulations, the glycosidic linkage of this compound seems to be more rigid than those of its analogues, as observed in different 3-*O*-substituted lactose or lactosamine fragments[28]. The effects of alkylation for C-3′ and C-4′ agree fairly well with the observations of Angyal and Odier for *O*-methylation on one equatorial oxygen (O-3′) flanked by atoms bearing one equatorial and one axial hydroxyl and for *O*-methylation on one axial oxygen (O-4′) whose adjacent carbon atoms carry equatorial substituents. In the first case (**6**), only H-4′ and C-4′ are importantly affected in both solvents, indicating that the methyl group preferentially adopts the orientation 1,3-parallel to H-4′, while, in the second case (**7**), the observed shifts indicate that the two possible orientations of the methyl group pointing out of the pyranoid ring coexist in solution.

Hydroxymethyl conformation.—Glucose and galactose H-6*pro-R* and H-6*pro-S* were assigned as previously reported for similar derivatives[16,35]. The distribution of rotamers was calculated for those compounds which showed resolved couplings for H-5 (Table VII) and/or the corresponding H-6s, following well-established methodology[36] by using the Karplus–Altona[37] equation and assuming *gg* : *gt* and *gt* : *tg* equilibria for the glucose and galactose residues, respectively[14,16,38]. The observed

couplings for the lateral chain of the different glucose residues can be explained for ca. 60:40 (±5) distributions of *gg* and *gt* rotamers. On the other hand, the values observed for the D-galactopyranose moieties agree with combinations of the *gt* and *tg* rotamers, with the *gt* family populated[38] ≥ 65%. The distribution of rotamers is basically the same in both solvents, indicating that the polarity of D_2O and Me_2SO-d_6 precludes the existence of the *tg* and *gg* rotamers for glucose and galactose, respectively. These rotamers could be stabilized by an intramolecular hydrogen bond between O-4 and O-6, as observed in molecular dynamics simulations in vacuo[39].

Analysis of NOE data.—An important problem for the conformational analysis of the lactose-type of disaccharide is the problem of strong overlap among H-3, H-4, and, in some cases, H-3′ nuclei with potential NOE to H-1′. Nevertheless, the use of a specifically deuterated derivative of **1** showed[9,31] that the NOE to H-3 is practically nonexistent, a fact corroborated indirectly with several deoxy analogues of **1**[1,31]. In the case of the *O*-methyl derivatives presented in this study, H-4 does not overlap with H-3 in compounds **3** and **5–7** in D_2O, and in **2–4** in Me_2SO-d_6 solution. Besides, the NOESY and ROESY experiments alleviated the overlapping problem. In all these cases, no H-1′ to H-3 NOE was detected. In addition, for the other compounds, the problem may be resolved through the use of 2D-HSMQC-ROESY experiments, which allow the detection of NOEs, using the carbon frequencies to remove the proton frequency degeneracy. A similar experiment, 2D-HMQC-NOESY[14b], has been used recently in the structural analysis of a biantennary oligosaccharide. However, due to their correlation times, the smaller NOEs for disaccharides **1–8** prompted us to use rotating-frame NOEs to examine the possibility of H-1′–H-4 or H-1′–H-3 dipolar relaxation, but using the non-overlapping C-3 and C-4 ^{13}C NMR frequencies to label the cross-peak. An example of the experiment for compound **6** is given in Fig. 6. The presence of H-1′/C-4, H-1′/C-5′, and H-1′/C-3′ connectivities can be noted as well as the intraresidue H-1/C-3 and H-1/C-5 for the glucose ring. Therefore, it can be concluded that no important cross-relaxation between H-1′ and H-3 does exist. Besides, the presence of NOE between H-1′ and H-4 and not between H-2′ and H-4 implies that compounds **1–8** spend most of their time in the low-energy region defined by local minima A, B, C, and C′. The differentiation among these minima is more difficult since their expected interresidue contacts are very similar. Nevertheless, the presence of NOE between H-1′ and the H-6s indicates that the region defined by conformer A is populated to some extent. However, the fast equilibrium between the *gg* and *gt* rotamers with a different correlation time to that of the overall motion implies that the exact value of this NOE is very difficult to simulate. An estimation of interresidue distances may be obtained by the use of the isolated spin-pair approximation (ISPA), using the volumes of the cross-peaks between proton pairs in NOESY or ROESY spectra acquired with a relatively short mixing time (Table IX). This approximation leads to H-1′–H-4 distances in the range 2.2–2.5 Å, as expected for the low-energy region, without the possibility of

discrimination among the different conformers. The corresponding average distance for **1** from MD simulations is 2.49 Å, although oscillations between 2.1 and 2.9 Å could be observed. The ISPA approximation leads to average H-1′–H-6s distances lying between 3.0 and 3.5 Å, which also corresponds to the low-energy region. Nevertheless, a more rigorous approach for evaluation of the experimental data is to use the geometries of the different conformers for calculation of the expected NOEs[20–22] via a complete relaxation matrix approach[26–28] using either a single conformational model or an average[30] according to a Boltzmann distribution function at a given temperature[40–42]. The observed results are collected in Tables X–XIV. The correlation times for compounds **3**, **5**, and **6** were estimated from ^{13}C NMR T_1 measurements in both solvents at two different temperatures (Table XV). The observed average correlation times did not fit the values of the intraresidue NOEs in the glucose and galactose rings, which are basically conformation-independent and lead to smaller intensities than those found experimentally. A satisfactory match between the calculated and experimental intensities of H-1′–H-3′ and H-1′–H-5′ in steady-state measurements and in NOESY experiments, and of H-1–H-3 and H-1–H-5 in NOESY experiments was obtained by using average correlation times ca. 30–40% higher than those estimated from the ^{13}C NMR relaxation data. A similar situation has been found previously in several oligosaccharides[42–44]. The discrepancy could be due to the presence of anisotropic overall motion or to the existence of internal motions around the glycosidic linkages[43]. In fact, the observed relaxation times for C-4′ were ca. 15% smaller than those for the rest of the methine carbons, indicating a slight anisotropy of the overall motion. Besides, the relaxation times for C-6 and C-6′ showed that the internal motion around both lateral chains is rather different, the one for the glucose moiety being more hindered[14]. The comparison among the observed and calculated interresidue cross-peaks H-1′–H-4 and H-1′–H-6*proR,S* for the different individual conformers indicated that a satisfactory match was found by considering the presence of the different local minima A, B, C, and C′ in the conformational equilibrium in both D_2O and Me_2SO-d_6 since none of the individual conformers could match all the NOE values at the same time. The presence of conformers D or E to an appreciable extent can be discarded since they would produce H-1′–H-4 intensities noticeably smaller than those observed, along with observable NOE values for the H-1′–H-3 and/or H-2′–H-4 contacts that were never observed either in steady-state or NOESY/ROESY measurements. These results indicate that the extent of flexibility around the β-(1 → 4) linkage in compounds **1**–**8** in D_2O or Me_2SO-d_6 solutions is rather small, since the NMR data can be satisfactorily explained by considering contributions of conformers defined by $\Phi = -100 \pm 40°$ and $\Psi = -150 \pm 30°$. Therefore, only ca. 5% of the complete potential energy surface is populated in solution. Therefore, the recognition of conformers D or E should be accompanied by the formation of several hydrogen bonds or stabilizing van der Waals contacts to override the important energy barrier between the low-energy region and these islands. According to our

TABLE IX

Experimental 2D-CAMELSPIN (ROESY) cross-peaks at mixing time 350 ms for compounds **3**, **5**, and **6** at 37°C in D_2O, and 37 and 60°C in Me_2SO-d_6 solution

Compound	Cross-peak intensity (%)						
	H-1′/3′	H-1′/5′	H-1′/4	H-3′/4′	H-4′/5′	H-1/3	H-1/5
D_2O 37°C							
3	8 [a]	8 [a]	5	10 [b]	10 [b]	4	5
5	7 [a]	7 [a]	5	9 [b]	9 [b]	7 [c]	7 [c]
6	4	5	6	5	4	8 [a]	8 [a]
Me_2SO-d_6 37°C							
5	7 [a]	7 [a]	6	7 [b]	7 [b]	7 [c]	7 [c]
6	3	4	5	6 [b]	6 [b]	7 [a]	7 [a]
Me_2SO-d_6 60°C							
3	8 [a]	8 [a]	7	10 [b]	10 [b]	6 [c]	6 [c]
5	8 [a]	8 [a]	7	9 [b]	9 [b]	8 [c]	8 [c]
6	4	5	8	5	4	9 [a]	9 [a]

[a,b,c] Overlapping signals.

results, the glycosidic bonds of the *O*-methylated derivatives (**1–8**) of lactose are not as flexible as observed for the β-(1 → 4) linkage within the GM1 ganglioside[45] in Me_2SO-d_6, but closer to the conclusions reached recently for the same glycosidic bond in the GM3 analogue[27], the LeX trisaccharide[26,28], and 6′-*O*-sialyllactose[14,46]. In a previous study of selectively deuterated **1**, based on ^1H NMR T_1 measurements[47], it was concluded that the conformation of the β-(1 → 4) linkage can be defined by considering only conformation A.

TABLE X

Experimental and calculated steady-state NOEs for compounds **3**, **5**, **6**, and **8** at 37°C in D_2O solution upon saturation of the H-1′ signal

Compound	Observed NOE for signal (%)						
	H-2′	H-3′	H-4′	H-5′	H-4	H-6_R	H-6_S
3	5	7	−1.5	9	13	1	1
5	3	7	−1.5	10	13	0.5	0.5
6	4	6	−2	10	15	1	1
8	3	7	−1.5	10	15	1	1
	Calculated NOE (%) for compound **1** [a]						
	H-2′	H-3′	H-4′	H-5′	H-4	H-6_R	H-6_S
Conformer A	7	8	−1.3	10	18	2	−0.5
Conformer B	4	7	−1.0	10	13		
Conformer C	4	7	−1.3	10	17		
Conformer C′	5	8	−1.3	10	21		
Average	5	8	−1.2	10	17	0.5	

[a] Using the full-matrix relaxation method and $\tau_c = 0.10 \times 10^{-9}$ s. NOEs smaller than 1% are only approximate.

TABLE XI

Experimental and calculated steady-state NOEs for compounds **3** and **5–8** at 37°C in Me_2SO-d_6 solution upon saturation of the H-1′ signal

Compound	Observed NOE for signal (%)						
	H-2′	H-3′	H-4′	H-5′	H-4	H-6_R	H-6_S
3	2	3		6	7	0.5	0.5
5	3	4		5	8	0.5	0.5
6	3	2	−0.5	6	9	0.5	0.5
7	2	4		5	7	0.5	0.5
8	2	4		5	7		
	Calculated NOE (%) for compound **1** [a]						
	H-2′	H-3′	H-4′	H-5′	H-4	H-6_R	H-6_S
Conformer A	4	5	−0.3	5	8	0.5	
Conformer B	3	4	−0.3	5	7		
Conformer C	2	4	−0.3	5	7		
Conformer C′	4	4	−0.3	5	10		
Average	3	4	−0.3	5	8	0.2	

[a] Using the full matrix relaxation method and $\tau_c = 0.22 \times 10^{-9}$ s. NOEs smaller than 1% are only approximate.

Although a great area of the low-energy region matches the geometric requirements for the formation of an O-3–O-5′ hydrogen bond, the results obtained for the 3-*O*-methyl derivative **3** in both D_2O and Me_2SO-d_6 indicate that the formation of this hydrogen bond is not essential for the presence of A and B conformers

TABLE XII

Experimental and calculated steady-state NOEs for compounds **3–8** at 60°C in Me_2SO-d_6 solution upon saturation of the H-1′ signal

Compound	Observed NOE for signal (%)						
	H-2′	H-3′	H-4′	H-5′	H-4	H-6_R	H-6_S
3	3	5		8	12	0.5	0.5
4	4	6	−0.5	8	12	0.5	0.5
5	3	6	−0.5	8	13	0.5	0.5
6	2	5	−0.5	7	11	0.5	0.5
7	3	5		7	14		
8	4	6		7	12		
	Calculated NOE (%) for compound **1** [a]						
	H-2′	H-3′	H-4′	H-5′	H-4	H-6_R	H-6_S
Conformer A	6	7	−1	8	14	2	
Conformer B	4	6	−0.5	8	13		
Conformer C	3	6	−0.5	8	14		
Conformer C′	7	7	−1.0	8	18		
Average	5	6	−1.0	8	15	0.5	

[a] Using the full-matrix relaxation method and $\tau_c = 0.15 \times 10^{-9}$ s. NOEs smaller than 1% are only approximate.

TABLE XIII

Experimental and calculated NOESY intensities (mixing time, 0.7 s) for compounds **3**, **5**, and **6** at 37°C in D_2O solution

Compound	Cross-peak intensity (%)						
	H-1′/3′	H-1′/5′	H-1′/4	H-3′/4′	H-4′/5′	H-1/3	H-1/5
3	7 [a]	7 [a]	6	9 [b]	9 [b]	3	4
5	7 [a]	7 [a]	6	9 [b]	9 [b]	7 [c]	7 [c]
6	3	4	5	4	4	6 [b]	6 [b]
	Calculated intensity (%) for compound **1** [d]						
	H-1′/3′	H-1′/5′	H-1′/4	H-3′/4′	H-4′/5′	H-1/3	H-1/5
Conformer A	2.3	3.6	5.3	4.2	3.4	2.2	3.5
Conformer B	2.4	3.7	4.9	4.2	3.4	2.3	3.6
Conformer C	2.4	3.7	5.8	4.2	3.4	2.3	3.6
Conformer C′	2.3	3.5	6.4	4.2	3.4	2.2	3.4
Average	2.3	3.6	5.6	4.2	3.4	2.2	3.5

[a,b,c] Overlapping signals. [d] Using the full-matrix relaxation method and $\tau_c = 0.10 \times 10^{-9}$ s.

TABLE XIV

Experimental and calculated NOESY intensities (mixing time, 0.7 s) for compounds **3** and **6** at 37 and 60°C in Me_2SO-d_6 solution

Compound	Cross-peak intensity (%)						
	H-1′/3′	H-1′/5′	H-1′/4	H-3′/4′	H-4′/5′	H-1/3	H-1/5
Temperature 60°C							
3	5 [a]	5 [a]	5	6 [b]	6 [b]	4 [c]	4 [c]
6	2	3	5	3	3	5 [b]	5 [b]
Temperature 37°C							
3	1	2	4	5 [b]	5 [b]	4 [a]	4 [a]
	Calculated intensity (%) for compound **1** [d]						
	H-1′/3′	H-1′/5′	H-1′/4	H-3′/4′	H-4′/5′	H-1/3	H-1/5
Conformer A	2.1	3.1	4.6	3.7	3.0	2.1	3.1
Conformer B	2.1	3.2	4.3	3.7	3.0	2.1	3.1
Conformer C	2.1	3.1	5.0	3.7	3.0	2.1	3.1
Conformer C′	2.0	3.0	5.5	3.7	3.0	2.1	3.1
Average	2.1	3.1	4.9	3.7	3.0	2.1	3.1
	Calculated intensity (%) for compound **1** [e]						
	H-1′/3′	H-1′/5′	H-1′/4	H-3′/4′	H-4′/5′	H-1/3	H-1/5
Conformer A	1.3	2.1	3.2	2.6	2.0	1.3	2.1
Conformer B	1.3	2.2	3.0	2.6	2.0	1.3	2.1
Conformer C	1.3	2.2	3.5	2.6	2.0	1.3	2.1
Conformer C′	1.3	2.1	3.8	2.6	2.0	1.3	2.1
Average	1.3	2.1	3.3	2.6	2.0	1.3	2.1

[a,b,c] Overlapping signals. [d] Using the full-matrix relaxation method and $\tau_c = 0.15 \times 10^{-9}$ s. [e] Full-matrix relaxation and $\tau_c = 0.22 \times 10^{-9}$ s.

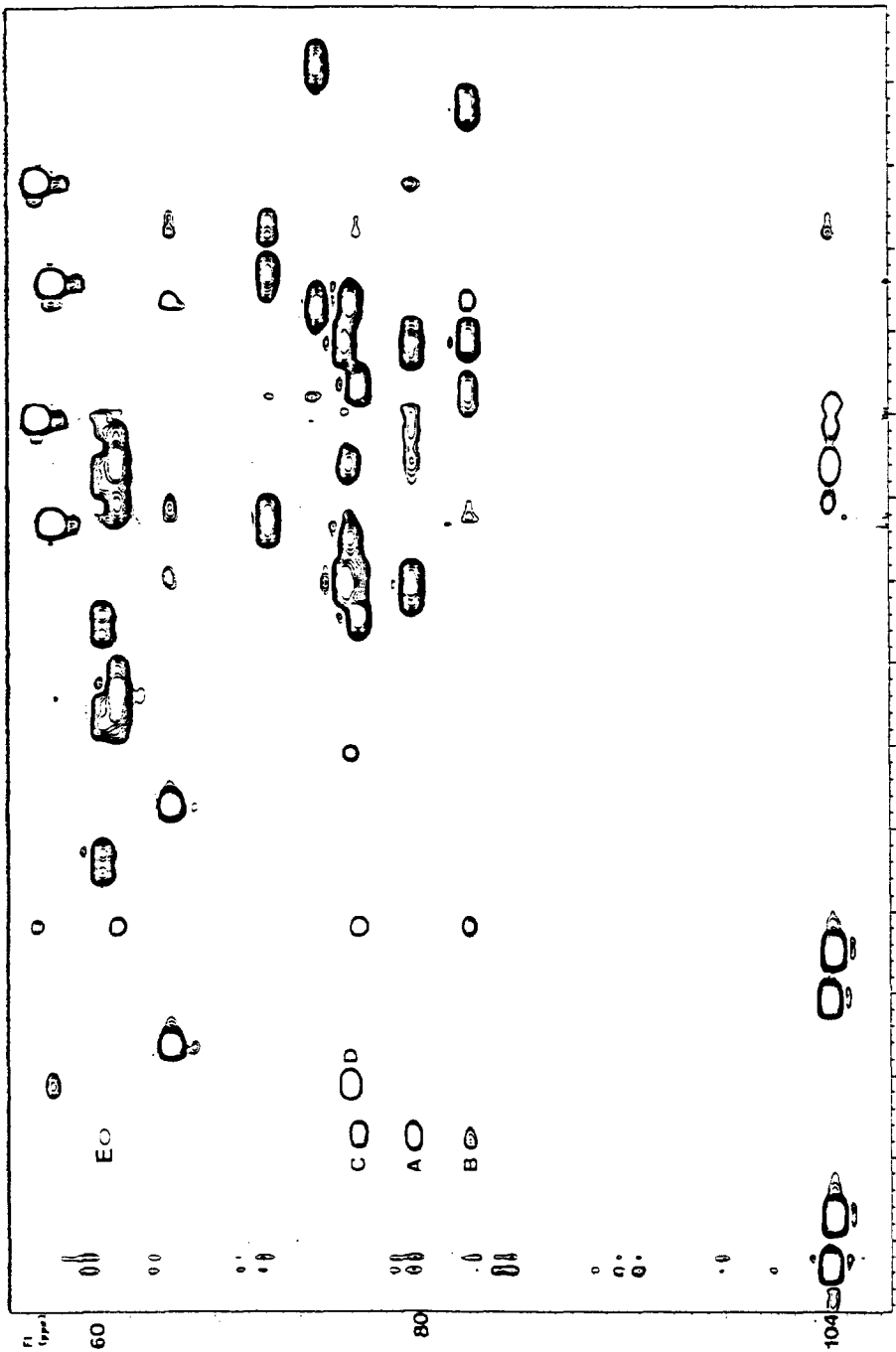

Fig. 6. HSMQC-ROESY spectrum (300 ms) at 37°C of compound **6** in D_2O. Relevant cross-peaks are marked. A, H-1′–C-4; B, H-1′–C-3′; C, H-1′–C-5′; D, H-1–C-3/C-5; E, H-1′–C-6. No cross-peaks between H-1′ and C-3 or C-5 are observed.

TABLE XV

Experimental average methine ^{13}C NMR relaxation times (T_1, s) and corresponding average correlation times (τ, 10^{-9} s) for compounds **3**, **5**, and **6** in D_2O at 37°C and Me_2SO-d_6 at 37 and 60°C

Compound	Solvent					
	D_2O		Me_2SO-d_6 (37°C)		Me_2SO-d_6 (60°C)	
	T_1	τ_c	T_1	τ_c	T_1	τ_c
3	0.69	0.08	0.41	0.14	0.61	0.09
5	0.73	0.07	0.45	0.13	0.65	0.08
6	0.72	0.07	0.43	0.13	0.63	0.09

to an important extent. The MD calculations for **1**, **3**, and **5** produced average O-5′–O-3 distances of 2.95 ± 0.10 Å. In fact, although the existence of the corresponding hydrogen bond in methyl β-cellobioside has recently been demonstrated in Me_2SO-d_6, there are contradictory results for D_2O solutions since, for methyl β-cellobioside, it has been reported to disappear in aqueous solution, at least for most of the time[33]. On the other hand, it has been postulated to exist in 6′-*O*-sialyllactose[46]. Therefore, it may be concluded that compounds **1–8** show a very similar solution conformation, since all the experimental data can be described by a conformational equilibrium of the conformers included in the low-energy region A-C′, as calculated from molecular mechanics and dynamics methods. Assuming that the interaction with the lectin takes place in one of these conformations[9], the observed dissociation constants may be used to correlate structure and activity.

ACKNOWLEDGMENTS

We thank Professor M. Bernabé and Dr. A. Rivera (Madrid) for helpful discussions, Dr. M. Forster (Potters Bar, UK) for the use of the NOEMOL programme, Dr. A. Imberty (Nantes, France) for a preprint of ref 24 prior to publication, and Professor M. Martín-Lomas for his continuous interest and support. Financial funding from Dirección General de Investigación Científica y Técnica (grant PB-870367) is gratefully acknowledged.

REFERENCES

1 A. Rivera-Sagredo, D. Solis, T. Diaz-Mauriño, J. Jiménez-Barbero, and M. Martín-Lomas, *Eur. J. Biochem.*, 197 (1991) 217–228.
2 A. Rivera-Sagredo, D. Solis, T. Diaz-Mauriño, J. Jiménez-Barbero, and M. Martín-Lomas, *Carbohydr. Res.*, 232 (1992) 207–226.
3 R.U. Lemieux, L.T.J. Delbaere, H. Beierbeck, and U. Spohr, *Ciba Found. Symp.*, 158 (1990).
4 C.P.J. Glaudemans, *Chem. Rev.*, 91 (1991) 25–33.
5 (a) K. Adelhorst, K. Bock, H. Pedersen, and S. Refn, *Acta Chem. Scand., Ser. B*, 42 (1988) 196–201; (b) J. Kihlberg, S.J. Hultgren, S. Normark, and G. Magnusson, *J. Am. Chem. Soc.*, 111 (1989) 6364–6368.
6 P.S. Vermersch, J.J.G. Tesmer, and F.A. Quiocho, *J. Mol. Biol.*, 226 (1992) 923–929.

7 P.V. Nikrad, H. Beierbeck, and R.U. Lemieux, *Can. J. Chem.*, 70 (1992) 241–253.
8 D. Solis, P. Fernández, T. Diaz-Mauriño, J. Jiménez-Barbero, and M. Martín-Lomas, *Eur. J. Biochem.*, in press.
9 V.L. Bevilacqua, D.S. Thomson, and J.H. Prestegard, *Biochemistry*, 29 (1990) 5529–5537.
10 V.L. Bevilacqua, Y. Kim, and J.H. Prestegard, *Biochemistry*, 31 (1992) 9339–9349.
11 C. Griesinger, G. Otting, K. Wüthrich, and R.R. Ernst, *J. Am. Chem. Soc.*, 110 (1988) 7870–7872.
12 (a) A.A. Bothner-By, R.L. Stephens, J.-M. Lee, C.D. Warren, and R.W. Jeanloz, *J. Am. Chem. Soc.*, 106 (1984) 811–813; (b) A. Bax and D.G. Davis, *J. Magn. Reson.*, 63 (1985) 207–213.
13 H. Kessler, C. Griesinger, R. Kerssebaum, K. Wagner, and R.R. Ernst, *J. Am. Chem. Soc.*, 109 (1987) 607–609.
14 J. Breg, L.M.J. Kroon-Batenburg, G. Strecker, J. Montreuil, and J.F.G. Vliegenthart, *Eur. J. Biochem.*, 178 (1989) 727–739.
15 (a) A. Bax and S. Subramanian, *J. Magn. Reson.*, 67 (1986) 565–569; (b) E.R.P. Zuiderweg, *ibid.*, 86 (1990) 346–357.
16 (a) Y. Nishida, H. Ohrui, and H. Meguro, *Tetrahedron Lett.*, 25 (1984) 1575–1578; (b) D.M. Mackie, A. Maradufu, and A.S. Perlin, *Carbohydr. Res.*, 150 (1986) 23–33.
17 A.T. Hagler, S. Lifson, and P. Dauber, *J. Am. Chem. Soc.*, 101 (1979) 5122–5130.
18 Discover 2.8 Program, Biosym Technologies Inc., San Diego, CA, USA.
19 Insight 2.1.0 Program, Biosym Technologies Inc., San Diego, CA, USA.
20 T. Peters, J.R. Brisson, and D.R. Bundle, *Can. J. Chem.*, 68 (1990) 979–988, and references therein.
21 (a) M. Forster, C. Jones, and B. Mulloy, *J. Mol. Graph.*, 7 (1989) 196–201; (b) M.J. Forster, *J. Comput. Chem.*, 12 (1991) 292–300.
22 D. Neuhaus and M.P. Williamson, *The Nuclear Overhauser Effect in Structural and Conformational Analysis*, VCH, New York, 1989.
23 M. Bernabé, A. Fernández-Mayoralas, J. Jiménez-Barbero, M. Martín-Lomas, and A. Rivera-Sagredo, *J. Chem. Soc., Perkin Trans. 2*, (1989) 1575–1578.
24 A. Imberty, Y. Bourne, C. Cambillau, P. Rouge, and S. Perez, *Adv. Biophys. Chem.*, in press.
25 Y. Bourne, P. Rouge, and C. Cambillau, *J. Biol. Chem.*, 267 (1992) 197–203.
26 (a) S.W. Homans, *Biochemistry*, 29 (1990) 9110–9118; (b) S.W. Homans and M. Forster, *Glycobiology*, 2 (1992) 143–151.
27 (a) H.C. Siebert, G. Reuter, R. Schauer, C.W. von der Lieth, and J. Dabrowski, *Biochemistry*, 31 (1992) 6962–6971; (b) A.E. Aulabaugh, R.C. Crouch, G.E. Martin, A. Ragouzeos, J.P. Shockcor, T.D. Spitzer, R.D. Farrant, B.D. Hudson, and J.C. Lindon, *Carbohydr. Res.*, 230 (1992) 201–212.
28 K.E. Miller, C. Mukhopadhyay, P. Cagas, and C.A. Bush, *Biochemistry*, 31 (1992) 6703–6709.
29 K. Bock, *Pure Appl. Chem.*, 55 (1983) 605–622.
30 K. Bock, H. Lönn, and T. Peters, *Carbohydr. Res.*, 198 (1990) 375–380.
31 A. Rivera-Sagredo, J. Jiménez-Barbero, and M. Martín-Lomas, *Carbohydr. Res.*, 221 (1991) 37–47.
32 K. Hirotsu and A. Shimada, *Bull. Chem. Soc. Jpn.*, 47 (1974) 1872–1879.
33 B.R. Leeflang, J.F.G. Vliegenthart, L.M.J. Kroon-Batenburg, B.P. van Eijck, and J. Kroon, *Carbohydr. Res.*, 230 (1992) 41–61.
34 S.J. Angyal and L. Odier, *Carbohydr. Res.*, 123 (1983) 23–29.
35 Y. Nishida, H. Hori, H. Ohrui, and H. Meguro, *J. Carbohydr. Chem.*, 7 (1988) 239–250.
36 R.J. Abraham, E.J. Chambers, and W.A. Thomas, *Carbohydr. Res.*, 226 (1992) c1–c5.
37 C.A.G. Haasnoot, F.M. de Leeuw, and C. Altona, *Tetrahedron*, 36 (1980) 2783–2792.
38 K. Bock and S. Refn, *Acta Chem. Scand., Ser. B*, 41 (1987) 469–472.
39 L.M.J. Kroon-Batenburg and J. Kroon, *Biopolymers*, 29 (1990) 1243–1248.
40 D.A. Cumming and J.P. Carver, *Biochemistry*, 26 (1987) 6664–6676.
41 A. Imberty, V. Tran, and S. Perez, *J. Comput. Chem.*, 11 (1989) 205–216.
42 P. Cagas and C.A. Bush, *Biopolymers*, 30 (1991) 1123–1138.
43 M. Hricovini, R.N. Shah, and J.P. Carver, *Biochemistry*, 31 (1992) 10018–10023.
44 S. Sabesan, J.O. Duus, T. Fukunaga, K. Bock, and S. Ludvigsen, *J. Am. Chem. Soc.*, 113 (1991) 3236–3246.
45 L. Poppe, C.W. von der Lieth, and J. Dabrowski, *J. Am. Chem. Soc.*, 112 (1990) 7762–7771.
46 L. Poppe, R. Stuike-Prill, B. Meyer, and H. van Halbeek, *J. Biomol. NMR*, 2 (1992) 109–136.
47 P.C. Kline, A.S. Serianni, S.G. Huang, M. Hayes, and R. Barker, *Can. J. Chem.*, 69 (1990) 2171–2182.